DEVELOPMENT OF HIGH POWER TRANSFERRED ELECTRON EFFECT DEVICES FOR X-BAND AND Ku-BAND OSCILLATORS

BY

S. YEGNA NARAYAN AND A. R. GOBAT

DECEMBER 1968

Prepared under
CONTRACT NO. NAS 12-685

by
RCA ELECTRONIC COMPONENTS
Microwave Applied Research Laboratory
David Sarnoff Research Center
Princeton, New Jersey 08540

ELECTRONICS RESEARCH CENTER
NATIONAL AERONAUTICS AND SPACE ADMINISTRATION

NATIONAL AERONAUTICS AND SPACE ADMINISTRATION
ELECTRONICS RESEARCH CENTER
CAMBRIDGE, MA 02139

PLEASE REPLY TO CODE AMTP

DATE: March 4, 1969

TO : NASA Scientific and Technical
Information Facility
P. O. Box 33
College Park, Maryland 20740

FROM : AMTP/Acting Supervisor,
Technical Publications

SUBJECT: Transmittal of High Number
Contractor Report (CR-86116)

The enclosed report under Contract NAS 12- 685 is entitled "Development of High Power Transferred Electron Effect Devices for X-Band and Ku-Band Oscillators".

Dr. A. I. Grayzel , Technical Monitor, recommends dissemination as a high-number contractor report.

D. C. Pierce

D. C. Pierce

Enclosures:

1. Subject Report (2 copies)
2. Document Release Form

cc: DA/F. Hills
DL/J. Manning
AT/E. Hadge
MIT/Capt. M. R. Jensen, AFSC/STLO

DEVELOPMENT OF HIGH POWER TRANSFERRED ELECTRON EFFECT DEVICES FOR X-BAND AND Ku-BAND OSCILLATORS

BY

S. YEGNA NARAYAN AND A. R. GOBAT

DECEMBER 1968

Prepared under

CONTRACT NO. NAS 12-685

by

RCA ELECTRONIC COMPONENTS
Microwave Applied Research Laboratory
David Sarnoff Research Center
Princeton, New Jersey 08540

ELECTRONICS RESEARCH CENTER
NATIONAL AERONAUTICS AND SPACE ADMINISTRATION

TABLE OF CONTENTS

LIST OF ILLUSTRATIONS

SUMMARY

Research program on cw transferred electron oscillators in X- and Ku-bands is described. Details of the material used, fabrication techniques, and characteristics of the oscillators delivered to the contracting agency are discussed. After analyzing the material and device technology available at the end of the contract, recommendation for further investigations are made.

INTRODUCTION

The purpose of this program is to develop cw transferred electron oscillators (Gunn oscillators) operating at X- and Ku-band frequencies. The objectives are: (1) a design goal of 50-200 mW at X-band and 15-60 mW at Ku-band, and (2) to analyze the material and device technologies available at the end of the program to determine whether further investigations leading to the development of transferred electron oscillators with power outputs as high as 500 mW at X-band and 150 mW at Ku-band are feasible.

This research program was successfully carried out. The design goals on the power output were achieved. Fourteen transferred electron devices were delivered to the contracting agency as per contract requirements. After analyzing the material and device technologies available at the completion of the program we conclude that further investigations with design goals of 500 mW at X-band and 150 mW at Ku-band are both feasible and promising. This future effort should be aimed at: (1) improving the device technology to achieve better heat sinking of the devices and (2) a theoretical and experimental study of circuit optimization.

SYMBOLS

n	Carrier concentration of the active layer
ℓ	Length of the active n layer
μ	Low field Hall mobility of the active n layer
P_{out}	Output power of the transferred electron oscillator
f	Operating frequency of the transferred electron oscillator.

TECHNICAL DISCUSSION

Material Growth

The GaAs required for this program was grown by epitaxial deposition from the vapor phase using the RCA vapor hydride synthesis technique. The GaAs wafers were grown on n+ GaAs substrates in the n+ - n - n+ configuration. The specifications for the active length ℓ and carrier concentration n of the active region are determined by the following requirements:

1. The transferred electron oscillators developed in this program operate in a travelling domain mode and hence ℓ is determined by the frequency of operation. Thus for X-band operation the required active length is between 9 microns to 12 microns while for Ku-band operation, ℓ is between 5 microns to 8 microns.
2. The optimum $n\ell$ product for efficient operation has been estimated to be 2×10^{12} cm^{-2} (Ref. 1). This, along with requirement 1, then determines the value of n required. The value of n required for this program is thus $2 - 5 \times 10^{15}$ cm^{-3}.

The characteristics of a few of the wafers used to fabricate devices for this program are summarized in Table I.

TABLE I

CHARACTERISTICS OF EPITAXIAL GaAs WAFERS

Wafer No.	Length of n layer-μm	n, cm^{-3} 300°K	μ cm^2/volt sec 300°K	n, cm^{-3} 77°K	μ cm^2/volt sec 77°K
188 Hall sample	Thick layer	2.24×10^{15}	8200	1.93×10^{15}	46,500
189 B n+ - n - n+	8	3×10^{15}*			
214 B n+ - n - n+	11	2.1×10^{15}*			
218 Hall sample	Thick layer	2.2×10^{15}	6750	2×10^{15}	38,000
219 A n+ - n - n+	10	1.7×10^{15}*			

The Ku-band devices were fabricated from wafer 189 B while the X-band devices were fabricated from wafer 214 B. The carrier concentration in the n+ - n - n+ structures were estimated from average resistivity and mobility data.

---

* Estimated from resistivity data.

Device Fabrication

The process used for the fabrication of transferred electron oscillators from an n+ - n - n+ sandwich wafer is described. This process is a batch process and a large number of devices are fabricated at one time. The geometry of the device is under excellent control and the evaluation of the devices also yields important information on the uniformity of the wafer. The fabrication process is summarized below with reference to Figure 1.

(1) The n+ - n - n+ wafer is taken from the reactor and small strips from both the leading and trailing edges are cleaved off. These strips are then stained with a copper etch and viewed on end under a high power (x 1000) microscope. The etch stains the layers of different resistivities to varying degrees and one can thus measure the thickness of the various layers. A photograph of such a stained strip is shown in Figure 2, where the top n+ layer is seen to be 6 microns while the active n layer is 8 microns. Note the sharp boundaries at the interfaces.

(2) A chip of suitable size, [Figure 1(a)] usually 0.250" x 0.250" is diced off the wafer and cleaned in organic solvents.

(3) The cleaned wafer is taken to an evaporator and silver dots are evaporated onto the n+ layer through a mask. These dots form ohmic contacts to the top n+ layer. After the deposition of the silver contacts the chip is sintered in an inert atmosphere. [Figure 1(b)]

(4) After sintering a few thousand angstroms of silicon dioxide is deposited over the chip. This process is done at a relatively low temperature of 400-450°C. [Figure 1(c)]

(5) Etch resistant masks of SiO_2 are defined around the silver dot by standard photo masking techniques. [Figure 1(d) and 1(e)]

(6) The chip is then etched to form a large number of mesa structures. [Figure 1(f)] The etch depth is determined by the thickness of the n and

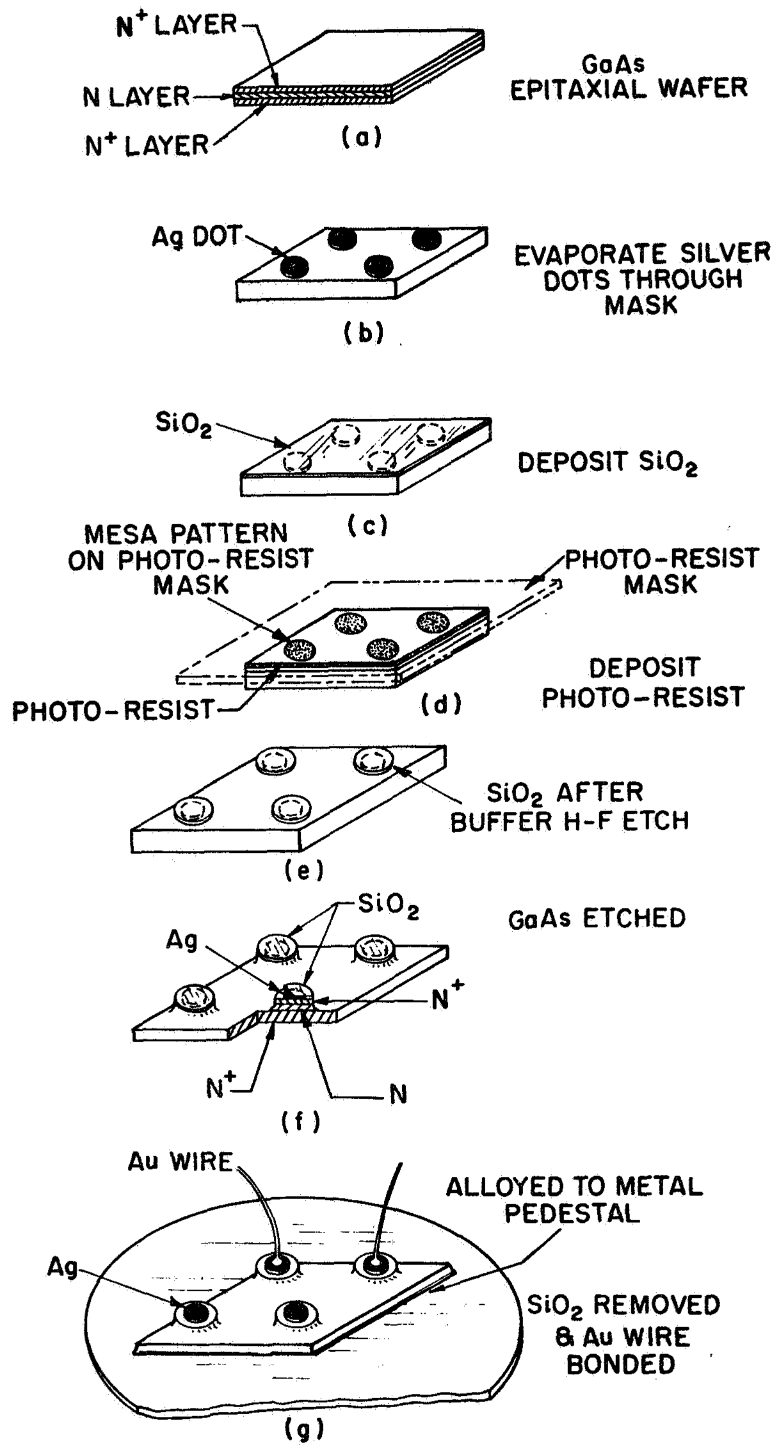

Figure 1 Batch process for fabrication of Transferred Electron Devices.

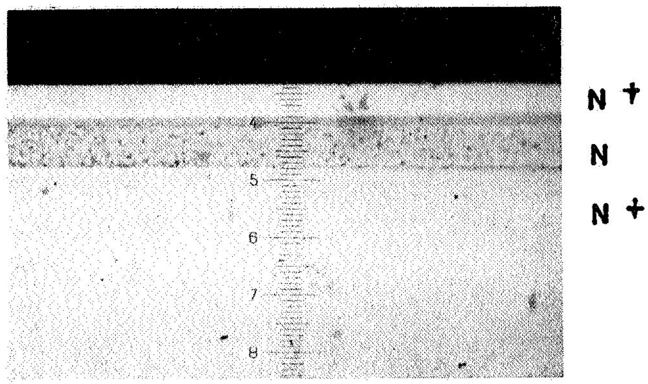

Figure 2 Cross-section of n+ - n - n+ GaAs wafer.
(x 1000, 1 small division = 1 micron)

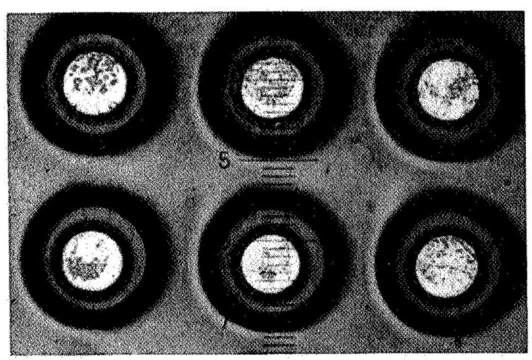

Figure 3 2 x 3 mesa array with SiO_2 mask after etching.
(x 200, 1 small division = 5 microns)

top n+ layers.

(7) The chip is then mounted on a handle with wax and the substrate lapped to a total chip thickness of 0.003 inches.

(8) After lapping, the chip is diced into small arrays of 2 x 2 or 3 x 3 mesas as required. Figure 3 shows a photograph of a 2 x 3 mesa array under a magnification of 200. Note that the etch depth and SiO_2 mask are clearly visible.

(9) The small mesa arrays are then alloyed to the pedestal of a standard varactor package. This process results in a strong mechanical connection, a good heat sink, and an ohmic contact to the substrate side of the chip.

(10) The SiO_2 masks on the silver contacts are then etched off and the alloyed chip cleaned in deionized water and thoroughly dried. Gold wires are bonded to the top of the mesas. This is shown in Figure 1(g) and a photograph of a four mesa device is shown in Figure 4. The device is now ready for both dc and rf testing.

Device Testing

The first test performed on a transferred electron device is the measurement of the dc current-voltage characteristic. The low field resistance, saturation voltage, and saturation current are measured. A photograph of the current-voltage characteristic of a typical device is shown in Figure 5. The characteristic is symmetric attesting to the uniformity of both the material and the contacting process. The devices exhibiting this characteristic current saturation of the transferred electron effect are then tested in an rf circuit.

The block diagram of the standard circuit used for rf tests is shown in Figure 6. The device is mounted in a tunable detector mount which has

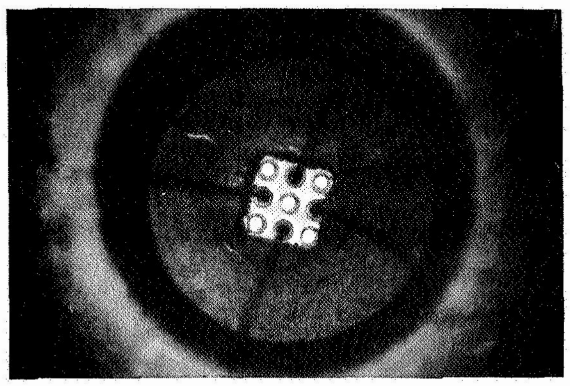

Figure 4 3 x 3 mesa array alloyed to package pedestal. Four mesas are connected by thermo-compression bonds.

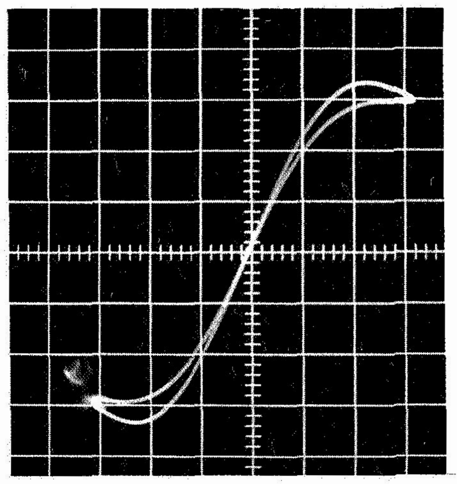

Figure 5 DC current-voltage characteristic of a typical TEO. Scale: x-axis 1 volt/division, Y-axis 100 mA/division.

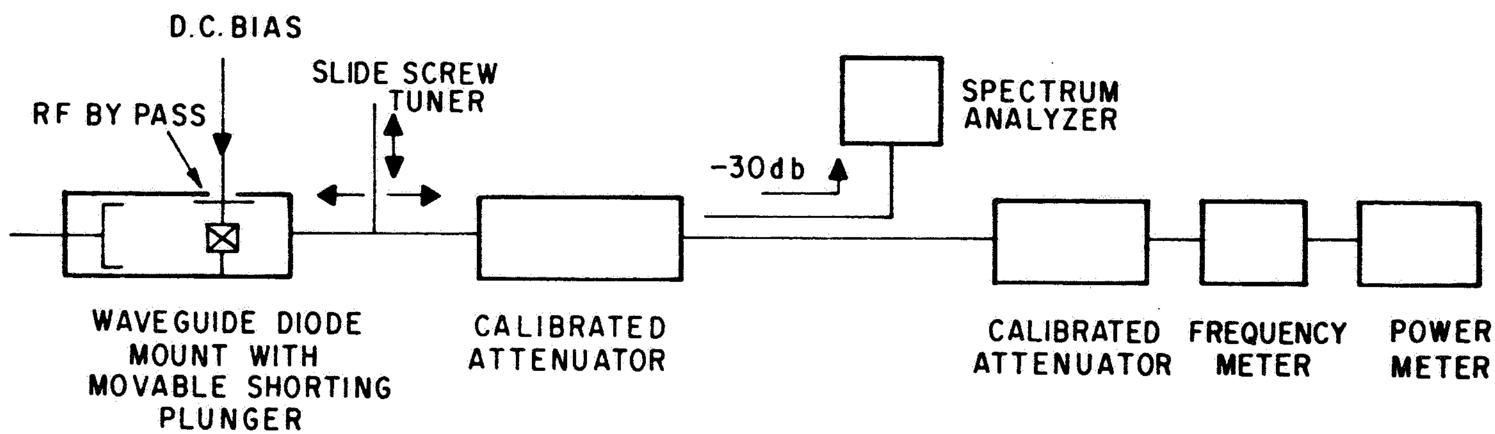

Fig. 6 Block diagram of rf test set-up.

a movable short circuit on one side of the device. On the other side of the device a slide screw tuner is connected. This movable short-slide screw tuner configuration forms a tunable resonant cavity with variable output coupling. The output power and the frequency spectrum are measured using standard techniques as shown in Figure 6. The X-band devices are tested in a circuit consisting of standard X-band waveguide while the Ku-band devices are tested in a Ku-band waveguide circuit.

The characteristics of the devices delivered to NASA-ERC are tabulated in Tables II and III. The power output of the devices lies in the range specified by the contract.

Ku-band oscillators

TABLE II

PERFORMANCE DATA OF Ku-BAND OSCILLATORS

Device No.	189C1	189C2	189C3	189C4	189B23	189B24
Low Field Resistance (ohms)	2.5	2.5	3.2	2.5	1.1	1.1
No. of Mesas	1	1	1	1	2	2
Operating Voltage	6.0	6.0	6.0	6.0	6.0	6.0
Operating Current (mA)	250	220	200	260	600	600
Power Output (mW)	40	35	17	50	130	130
Frequency (GHz)	13.7	14.1	13.2	13.8	12.7	13.0
Efficiency (%)	2.7	2.7	1.4	3.2	3.6	3.6

These frequency and power output data represent the values for optimum performance. The devices are easily tunable from below 12 GHz to over 16 GHz. 189B23 and 189B24 operate at the relatively high efficiency of 3.6% in an X-band waveguide circuit while they deliver only about 70 mW in a Ku-band circuit. All the other devices show their optimum performance in a Ku-band circuit and do not show any improvement in efficiency in an X-band circuit.

The reason for this behavior is not known. It is possible that 189B23 and 189B24 operate in the inhibited mode in the X-band circuit. The inhibited mode is believed to be a more efficient mode of operation.

X-band oscillators

TABLE III

PERFORMANCE DATA OF X-BAND OSCILLATORS

Device No.	214B1	214B3	214B5	214B6	214B11	214B12	214B13	214B16
Device Resistance (at 10 mA) (ohms)	2.0	2.1	2.0	1.9	1.2	1.8	2.4	0.8
No. of Mesas	2	2	2	2	3	2	2	4
Operating Voltage	8	8	8	8	7	7	8	7
Operating Current (mA)	500	450	450	500	750	500	400	1000
P_{out} (mW)	120	105	100	130	160	93	91	203
Frequency (GHz)	10.7	10.0	10.1	10.7	10.7	10.9	10.9	11.1
Efficiency (%)	3.0	2.9	2.8	3.3	3.0	2.7	2.9	2.9

All these measurements were made in an X-band waveguide circuit and as before, represent optimum performance points. All these devices are mechanically tunable from 9 to 11.5 GHz with lower power output.

The typical line width of these oscillators (3 dB linewidth) is a few KHz. Figure 7 is a photograph of a typical spectrum and shows the excellent line width.

Pulsed operation.- The only difference between pulsed and cw operation, insofar as the device is concerned, is that more dc power has to be dissipated under cw conditions. This increased power dissipation leads to a

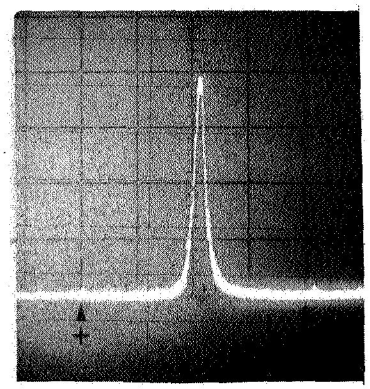

Figure 7 Spectrum of a typical TEO. Center frequency 10.7 GHz, Vertical axis 10 dB/division, horizontal axis 100 KHz/division.

higher operating temperature and consequently to lower efficiency. The lower power output and efficiency at higher operating temperature are a result of two factors. Firstly, since there is a maximum safe operating temperature for GaAs, less dc input power can be fed to the device, and secondly, the peak to valley ratio in GaAs decreases with increasing temperature. (Ref. 2) These facts are borne out by Figure 8. These measurements were made on a 0.005 inch diameter mesa oscillator at 14 GHz in a concurrent program on transferred electron oscillators. (Ref. 3) The power output and efficiency are plotted as a function of the duty cycle. It should be noted that the power output decreases from 800 to 41 mW while the efficiency decreases from 10% to 2.7%. This experiment shows that the low cw efficiency (3-4%) obtainable at present is due to temperature limitation. If the heat sinking of the devices can be improved, substantially better efficiency can be obtained at higher power levels.

Analysis of Results

Introduction.- The second objective of this contract is to analyze the material and device technologies available at the end of the program to determine whether further investigations leading to the development of devices with 500 mW output at X-band and 150 mW output at Ku-band are feasible. In this section we will discuss the results and show that such studies are indeed feasible.

Material Technology.- GaAs has now been grown on an almost continuous basis for this and other concurrent programs on transferred electron oscillators. The results of Hall measurements made on recently grown wafers is shown in Figures 9 and 10. The Hall mobility is plotted as a function of the carrier concentration at both 300°K and 77°K. The theoretical curve for the room temperature mobility (Ref. 4) is also shown. It should be observed that the experimental points are close to the theoretical curve attesting to the high quality of our GaAs. Carrier concentrations in the low 10^{15} cm^{-3}

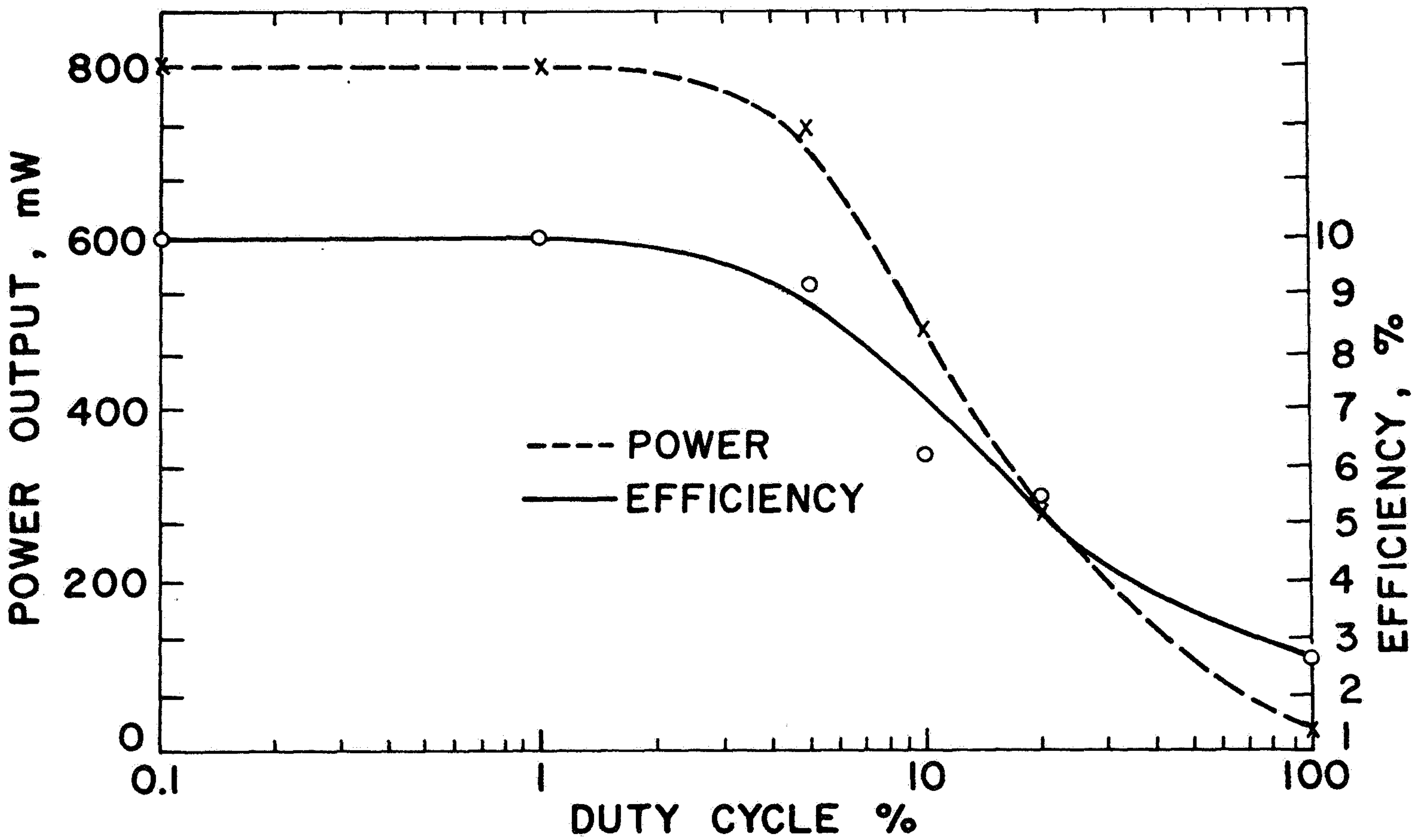

Figure 8 Power output and efficiency as a function of duty cycle. Pulse width 1 microsecond.

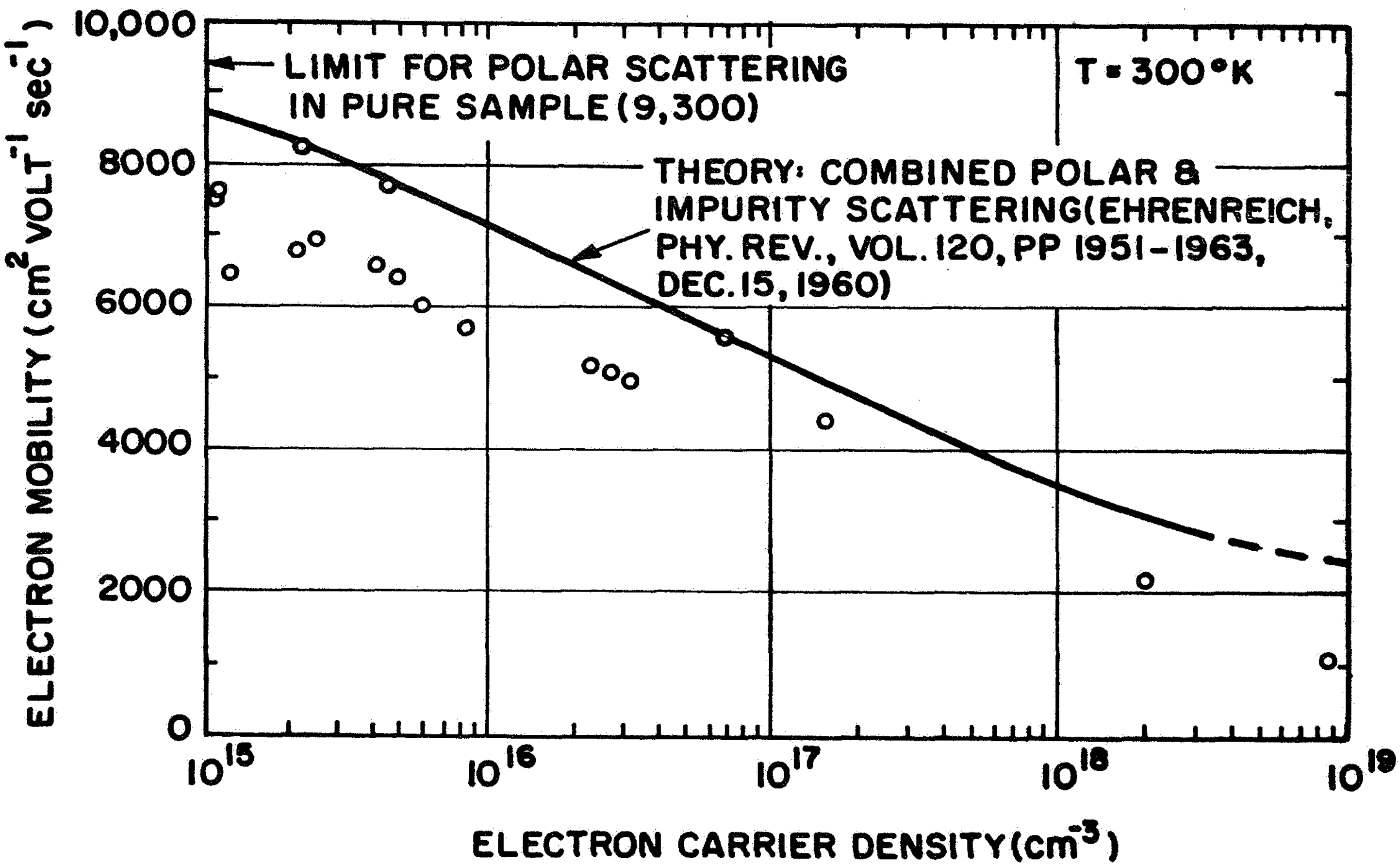

Fig. 9 Electron mobility as a function of carrier concentration for GaAs at 300°K.

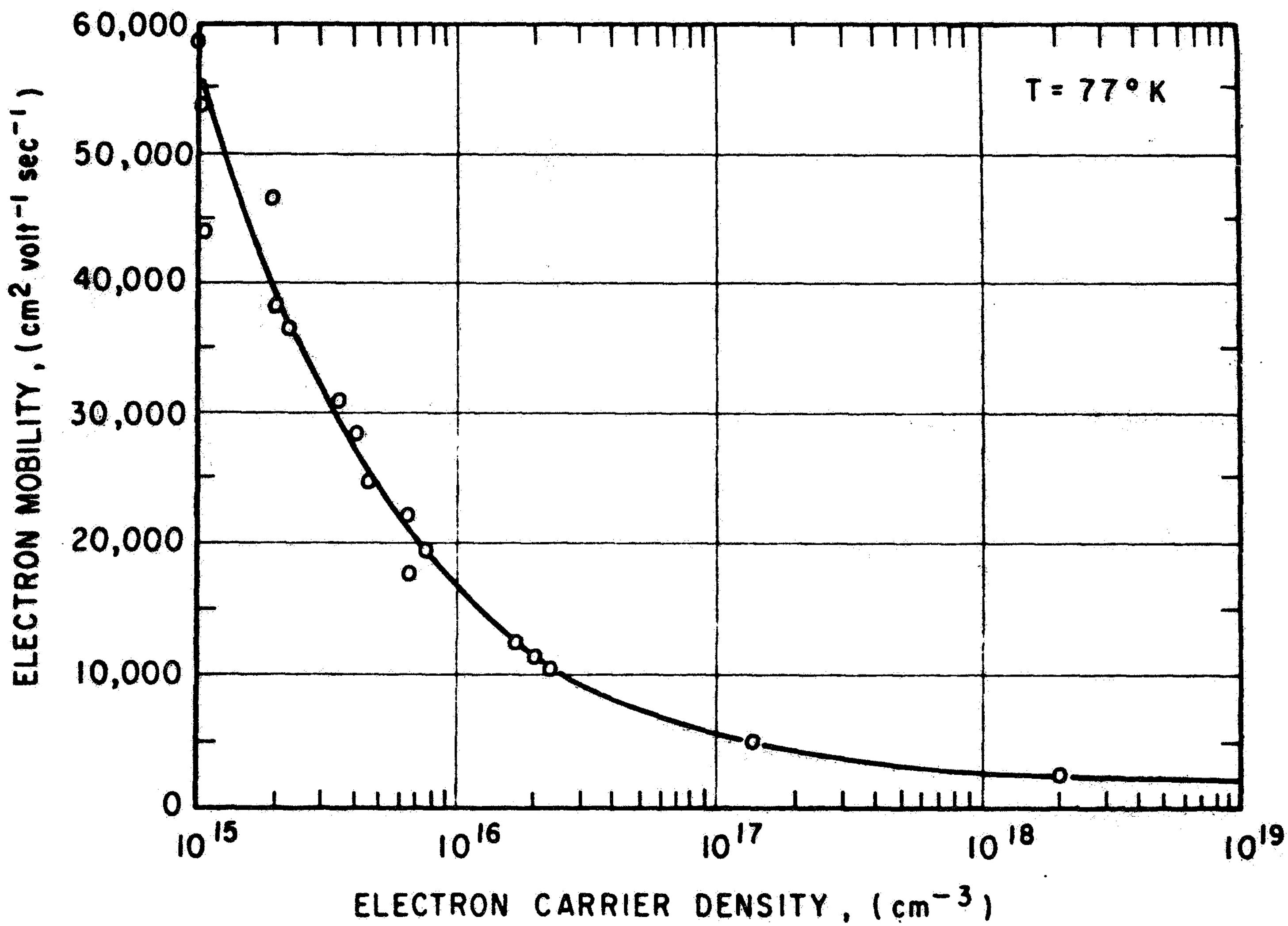

Fig. 10 Electron mobility as a function of carrier concentration for GaAs at 77°K.

(as required for X- and Ku-band devices) can now be obtained on a routine basis with almost the theoretical room temperature mobility. We believe that soon we will be in the mid 10^{14} cm^{-3} range and will rely on controlled back doping to obtain 2-5 x 10^{15} cm^{-3} required for X- and Ku-band operation. This will result in more uniformly doped wafers and should be conducive to high efficiency operation.

Device technology.- The device technology has now evolved to a stage where devices of 3-4% cw efficiency can routinely be fabricated on a batch process. As discussed in the section on device testing, these devices have potential for high efficiency operation if the device operating temperature can be kept low. This can be achieved by improving the heat sinking of the chips. In the current mounting scheme there is approximately 40 μ of n+ substrate between the heat sink and the active region which has an approximate thermal resistance of 25°C/watt. To achieve optimum operation the device mesas should be heat sunk from both top and bottom and the thickness of material between the active region and heat sink substantially reduced. This obvious step is not technologically trivial but must be solved for optimum performance. Improvement in heat sinking should, at the very least, double the efficiency which makes 500 mW cw at X-band a very realistic value.

Oscillator circuits.- All the results quoted in this report have been obtained using a basic circuit as shown in Figure 6 in either X- or Ku-band waveguide configuration. This is a very convenient and flexible circuit for quick evaluation of devices but there is reason to believe that this is not the best circuit. Since a well understood equivalent circuit for transferred electron oscillators is not available it is difficult to design a good circuit. Furthermore, since this device is a nonlinear device, it is necessary to design a circuit which is optimum not only at the fundamental frequency but also at the harmonics. Preliminary investigations have shown that second harmonic tuning can almost double the oscillator efficiency.

It appears, therefore, that it is necessary to theoretically study the operation of transferred electron oscillators to determine the optimum loading at the fundamental and harmonic frequencies to synthesize the optimum circuit configuration. Such circuit studies should lead to further enhancement of the efficiency.

In conclusion, we feel that further investigations to develop devices with cw power outputs of 500 mW at X-band and 150 mW at Ku-band are both feasible and promising. This requires work in two main areas, viz, (1) improved heat sinking and (2) circuit optimization.

CONCLUSIONS

Research and development on high power cw transferred electron oscillators in X- and Ku-bands was successfully carried out. The design goals of 50-200 mW in X-band and 15-60 mW in Ku-band were achieved. Fourteen transferred electron oscillators were delivered to the contracting agency.

After an analysis of the material and device technologies available at the end of this research program, we conclude that further investigations leading to the development of oscillators with power outputs of 500 mW in X-band and 150 mW in Ku-band are both feasible and promising. This future effort should be aimed at (1) improvement of the device technology to achieve better heat sinking and (2) a theoretical and experimental study of oscillator circuits.

REFERENCES

1. Copeland, J. A.: Theoretical Study of a Gunn Diode in a Resonant Cavity. IEEE Trans. on Elec. Devices, ED-14, No. 2, February 1967.

2. McCumber, D. E. and Chynoweth, A. G.: Theory of Negative-Conductance Amplification and of Gunn Instabilities in "Two-Valley" Semiconductors. IEEE Trans. on Elec. Devices, ED-13, No. 1, January 1966.

3. Narayan, S. Y. and Gobat, A. R.: High Bias Voltage Operation of GaAs Transferred Electron Oscillators. Electronics Letters, Vol. 4, No. 23, 15 November 1968.

4. Ehrenreich, H.: Band Structure and Electron Transport of GaAs. Phys. Rev. 120, No. 6, December 15, 1960.

NEW TECHNOLOGY APPENDIX

After a diligent review of the work performed under this contract, it was found that no new innovation, discovery, improvement, or invention was made.